



Iron-clay as a reusable heterogeneous Fenton-like catalyst for decolorization of Acid Green 25

N.H.M. Azmi, V.M. Vadivelu, B.H. Hameed*

School of Chemical Engineering, Engineering Campus, Universiti Sains Malaysia, 14300 Nibong Tebal, Penang, Malaysia

Fax: +0645941013; email: chbassim@eng.usm.my

Received 1 May 2012; Accepted 21 May 2013

ABSTRACT

Decolorization of Acid Green 25 (AG25) was achieved by using Fe-Ipoh clay (Fe-IC) as catalyst on Fenton-like process. The catalyst was prepared by impregnation method and was characterized. The effect of various parameters such as catalyst calcination temperature and duration of time, pH, initial concentration of hydrogen peroxide (H_2O_2) and AG25, catalyst dosage, and reaction temperature was studied. The best performance of AG25 decolorization was found to be 95% after 2 h of reaction by using 1.25 g/L catalyst dosage of Fe-IC calcined at 500 °C for 6 h and 6.7 mM of H_2O_2 at pH 3. Besides, the developed catalyst also indicated an advantage of low iron leaching and ability for reuse up to three runs, with slightly reduced decolorization of AG25 from 95 to 93% at the same reaction time.

Keywords: Heterogeneous Fenton process; Reusability; Clay; Acid Green 25; Low ion leaching

1. Introduction

Water pollution can be caused by toxics and poisons which come in the form of chemicals, dyes, and heavy metals from sources like palm oil mills, irrigation systems, textile factories, and agricultural wastes. Such polluted water can affect plants, animals, and the ecosystem due to their carcinogenic, mutagenic, and low biodegradation effects [1,2]. Usually, wastewaters from industrial factories are recalcitrant to treat by physical, chemical, and biological systems which are conventional methods of treating wastewaters. Furthermore, these processes are efficient neither with physical-chemical methods which only transfer the contamination from one phase to another and causing secondary wastes, nor with biological processes, since

the constituents of such wastewaters contain non-biodegradable organic compounds [3].

As an alternative way to treat such wastewaters, advanced oxidation processes (AOPs) have been widely proposed, for the facts that the process is fast, operates at atmospheric pressure and ambient temperature, and economically viable [4]. AOP technologies involve the generation of hydroxyl radicals in sufficient quantities to oxidize organic compounds present in the wastewater. Among the AOPs is the Fenton reaction, a system which uses iron cations as catalysts that reacts with hydrogen peroxide to produce strong oxidizing radical, hydroxyl radicals. Common homogeneous Fenton system that employs high iron concentration demands secondary treatment before the treated water can be discharged to environment; this makes the process unattractive as it becomes more

*Corresponding author.

laborious, time consuming, and more expensive [5]. More so, homogeneous Fenton reaction needs up to 50–80 ppm of iron ions in solution, which is much higher than 5 ppm proposed by National Water Quality Standard for Malaysia [6].

Thus, many researchers have refocused on the application of heterogeneous Fenton system to overcome these drawbacks of homogeneous Fenton reaction. A number of heterogeneous catalysts such as SBA-15 [6], transition metal (Zn, Co, Cu, Fe and Mn) incorporated zeolite [7], alumina [8,9], clay [10], goethite [11], Iron molybdate ($\text{Fe}_2(\text{MoO}_4)_3$) [12], and carbon-support [13] have been found to be efficient for the degradation of wastewater. Heterogeneous Fenton process involves the incorporation of Fe ions or Fe oxides into porous support.

In this study, a readily available and inexpensive large span of clay from Ipoh town in Perak state, Malaysia was used as heterogeneous catalyst support for the Fenton reaction. The use of clay as catalysts is due to its high chemical and mechanical stabilities, variety of surface and structural properties, high specific surface area, as well as its environmental friendliness [10]. Although clay have been widely used as catalytic supports and as catalysts, the reports of clay mineral used as heterogeneous Fenton catalyst especially from Malaysian sources were still rare in wastewater treatment to the best of our knowledge. Acid Green 25 (AG25), a commercial acid dye which is the largest and most important class of synthetic organic dyes often used in textiles, hair dye formulations, cosmetic products dyeing wool, silk, nylon, leather, and also to some extent in paper, food, and ink-jet printing, was used as a model pollutant [14]. This type of dyes is formed from chemical classes such as anthraquinone, azo, nitro, azine, nitroso, and xanthene which make them chemically stable and versatile. AG25 is a type of anthraquinonnic anionic dyes which is very difficult to decompose using common wastewater treatments due to the stability of anthraquinone moiety and their complex molecular structures and may cause mutagenic effects or even acute toxicity when exposed to living things [15]. Besides, the presence of dyes in water matrix can interfere with the growth of micro-organism and prevent photosynthesis in aquatic plants by absorbing and reflecting sunlight entering the water, which eventually leads to the destruction of aquatic life and indirectly threatens human life [16]. As a result, the wastewaters from industries are increasingly a major concern worldwide and need to be treated before being discharged into the environment.

The aim of this work was to investigate the applicability and performance of the Fe-Ipoh clay as

heterogeneous Fenton-type catalyst for the decolorization of AG25. The influence of operating conditions such as calcination temperature and duration of time, catalyst dosage, initial concentrations of the dye and H_2O_2 , and initial pH and temperature range is studied.

2. Materials and methods

2.1. Chemicals

Hydrogen peroxide (H_2O_2) (30%), ferric nitrate nanohydrate ($\text{Fe}(\text{NO}_3)_3 \cdot 9\text{H}_2\text{O}$), sodium carbonate (Na_2CO_3), sodium hydroxide (NaOH), and sulfuric acid (H_2SO_4) were of analytical grade and purchased from Merck Chemical, Malaysia. AG25 (75% of purity) with the empirical formula of $\text{C}_{28}\text{H}_{20}\text{N}_2\text{Na}_2\text{O}_8\text{S}_2$, a molecular weight of 622.58, and the maximum wavelength, $\lambda_{\text{max}} = 642 \text{ nm}$ was purchased from Sigma-Aldrich, Malaysia; all chemicals were used without further purification. The molecular structure of AG25 is shown in Fig. 12. The Ipoh clay (IC) used was obtained from Ipoh town in Perak state of Malaysia. The clay was washed several times with distilled water, dried in an oven at 100°C overnight, and then packaged in an air-tight container for further use.

2.2. Catalyst support material

The catalyst support used in this study is local natural clay taken from Ipoh, Perak, a state in Malaysia. Prior to use, at first, the support catalyst was powdered using a mortar and washed several times with distilled water to remove impurities. Then, the sample was dried in an oven at 100°C for 12 h. Finally, the dried sample was sieved to obtain a grain size of 63–75 μm .

2.3. Preparation of the catalyst

The heterogeneous catalyst, Fe-Ipoh clay (Fe-IC) was prepared by using impregnation method. In this process, 0.2 M of $\text{Fe}(\text{NO}_3)_3 \cdot 9\text{H}_2\text{O}$ was dissolved in a beaker containing distilled water and vigorously stirred before sodium carbonate was added, so that a molar ratio of 1:1 for $[\text{Na}^+]/[\text{Fe}^{3+}]$ was established [8]. Sodium carbonate was used as Na ions can be replaced by Fe^{3+} through a simple ion exchange reaction and hence increasing the possibility of Fe^{3+} to be attached to the support catalyst [16]. Then, 2 g of support powder, IC was added into the previous solution and was continuously stirred for 2 h followed by drying in an oven for 2 days at 80°C .

The dried solid was washed several times with distilled water to wash away excess Na ions and redried in an oven for 12 h at 80°C [8]. Lastly, the dried solid sample was calcined at a temperature range from 300 to 500°C for different duration times (4–6 h) in a muffle furnace [17] and labeled as Fe-IC300/4 (Fe-IC calcined at 300°C for 4 h).

2.4. Characterization of catalyst

The morphology of the IC and Fe-IC500/6 was studied using scanning electronic microscopy (SEM) (SEM-JEOL-JSM6301-F) with an Oxford INCA/Energy-350 microanalysis system.

The elemental chemical analyses were carried out using energy dispersive X-ray (EDX) spectroscopy to determine the elements of raw clay (IC) and Fe-IC500/6.

The Brunauer-Emmett-Teller (BET) surface areas (S_{BET}) were calculated from the corresponding nitrogen adsorption isotherms at 77 K using micrometrics model, ASAP 2020, 700VA, made in USA. volumetric analyzer. X-ray diffraction was used to investigate the X-ray diffraction patterns of the catalyst, mineral phase, and crystallinity before and after the impregnation process.

FT-IR spectra of IC and Fe-IC500/6 were recorded in the 4,000–400 cm^{-1} region with a PerkinElmer 1730 FT-IR spectrometer. He-Ne laser source was used to infrared the catalyst in KBr pellet. This technique was used to investigate the functional group presented at the surface of catalysts.

The total iron ions leached from the catalyst into the dye solution were determined right after the reaction was stopped using an atomic absorption spectrophotometer (AAS) model Shimadzu AA 6650. The analysis was carried out with the maximum absorbance wavelength of iron ion at 248.35 nm.

The total organic compound (TOC) was measured to evaluate the mineralization of AG25 using a Shimadzu 500A spectrophotometer, model TOC-500 CE.

2.5. Control experiments

To investigate whether the AG25 decolorization process occurred through catalytic reaction or adsorption or both processes, the effect of various parameters on the decolorization of AG25 was evaluated. The evaluation was administered through comparative experiments which were carried out in two different pH of solution: natural pH of AG25, pH 5.7 (without pH adjustment) and pH 3 to study the role of H_2O_2 , IC, and Fe-IC500/6 if they had any contribution to the

decolorization process in initial pH variation. In pH 5.7, experiments were done in the presence of only (1) H_2O_2 , (2) IC, and (3) Fe-IC500/6 while in pH 3 it was only in the presence of (4) H_2O_2 , (5) Fe-IC500/6, (6) Fe-IC500/6, and H_2O_2 .

2.6. Effect of catalyst calcination temperature and duration of time on the decolorization of AG25 and its reusability

To study the long-term stability of calcination temperature ranges and duration of time of Fe-IC catalysts, several experiments were run. 1.25 g/L of catalyst prepared at different calcination temperature and time duration was agitated in a thermostated water-bath shaker at 30°C, and at a shaker speed of 130 rpm for 1 h. The solution pH and H_2O_2 concentration were maintained at 3 and 6.7 mM, respectively. The catalyst was recovered from the solution through filtration, washed with distilled water, and dried at 100°C for 12 h in an oven. Leaching of iron ions from the catalyst into the dye solution was measured by AAS. The dried recovered catalyst was reused for the second run (R2) and third run (R3) at similar initial experimental conditions. The remaining concentration of AG25 at the end of each run was measured with UV-vis spectrophotometer.

2.7. Catalytic activity

The batch reaction was carried out in a set of 250-mL Erlenmeyer flasks containing 200 mL each of various initial dye concentrations (20–100 mg/L) which were placed in thermostated water-bath shaker at an agitation speed of 130 rpm for 2 h. Also, initial solution pH was adjusted to the desired value by using either 0.1 M H_2SO_4 or 0.1 M NaOH solution. The desired amounts of catalyst (0.75–1.75 g/L) were added into the flasks and the reaction commenced at the time when H_2O_2 was added. During the reaction, samples were withdrawn periodically and filtered to remove suspended particles. The concentration of AG25 was monitored with UV-vis spectrophotometer (Shimadzu, model UV 1601, Japan) at its maximum wavelength of 642 nm. The samples withdrawn were returned into the conical flasks to prevent any loss of content. The decolorization efficiency of AG25 was calculated as follows:

$$\text{Decolorization efficiency \%} = \left[1 - \frac{C_t}{C_0} \right] \times 100 \quad (1)$$

where C_0 (mg/L) is the initial concentration of AG25 and C_t (mg/L) is the concentration of AG25 at reaction time, t (min).

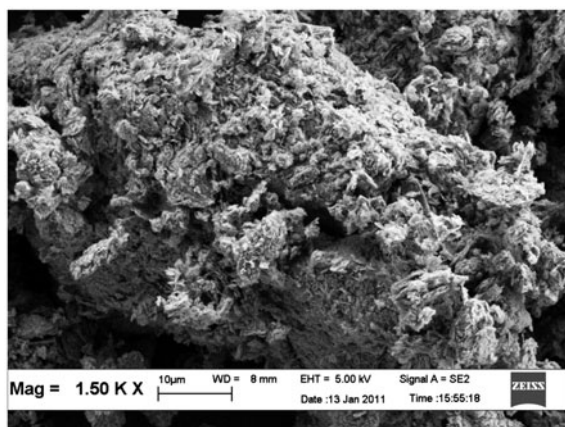
3. Results and discussion

3.1. Catalyst characterization

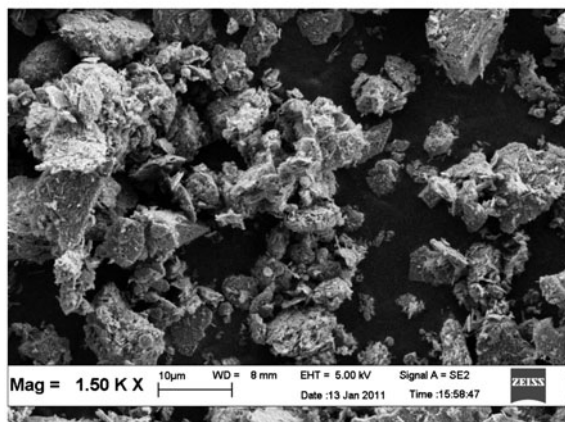
Fig. 1(a) and (b) show a SEM image of IC and Fe-IC500/6, respectively. The IC image shows a dense sheet with bigger particle sizes, while after treatment, the clay has become fluffy with random orientation. Such a fluffy appearance was attributed to the reduction in certain amorphous phases and change in the surface charge of the particle as a result of calcination process [18].

The BET surface area, pore volume, and pore size for IC and Fe-IC500/6 catalysts are $22.73 \text{ m}^2/\text{g}$, $0.121 \text{ cm}^3/\text{g}$, and 183.2 \AA , respectively.

The chemical compositions of IC and Fe-IC500/6 were measured by EDX and the results are shown in Table 1. EDX results further supported the impregna-



(a)



(b)

Fig. 1. SEM image of (a) IC and (b) Fe-IC500/6 (magnification: $1500\times$).

Table 1

EDX analysis of IC and Fe-IC500/6 catalyst

Element	IC Weight (%)	Fe-IC500/6 Weight (%)
O	44.46	35.28
Al	24.34	21.39
Si	26.91	26.31
K	3.02	1.81
Fe	1.27	15.21

tion of iron ions into the IC carried out by it increase from 1.27% (IC) to 15.21% (Fe-IC500/6).

Fig. 2 shows the wide angle XRD of IC and Fe-IC500/6. The main crystalline phases found in IC are quartz ($\alpha\text{-SiO}_2$), kaolinite ($\text{Al}_2\text{Si}_2\text{O}_5(\text{OH})_4$), and silicon oxide (SiO_2) with peaks at 12.5° , 21° and 25° , and 60° , respectively. It can be observed that the XRD patterns of Fe-IC500/6 almost coincided with the untreated IC. The Fe-IC500/6 maintained the layered structure in crystalline form with quartz and silicon oxide elements while peaks at 12.5° and 25° , corresponding to kaolinite disappeared after calcinations at 500°C ; this was due to the substitution of Fe on hydrated inter-layer cations [6]. The iron oxide phase observed is related to Fe_2O_3 crystallite (hematite) with $2\theta = 30.6^\circ$, 36.8° , 47.6° , and 69.7° [18]. These peaks are indicative of the presence of iron in the impregnated clay.

To identify the surface functional group of the IC and Fe-IC catalyst, FTIR analysis was used. The FTIR spectra were recorded at wavelength from $4,000$ to 400 cm^{-1} . The FTIR spectra of IC and Fe-IC500/6 are presented in Fig. 3. The bands at $3,697$, $3,621$ and $3,447 \text{ cm}^{-1}$ of the IC are assigned to the elongation vibration of hydroxyl group while the band at $3,447 \text{ cm}^{-1}$ is attributed to the O–H stretching of the silica group formed by the coupling molecules present in the surface of the clays. However, these bands were shifted and formed a broader band at $3,436 \text{ cm}^{-1}$ after calcinations at 500°C ; this indicated that water adsorbed on the clay surface was removed by calcinations [19], which was strongly supported by the deformation band at $1,637 \text{ cm}^{-1}$. In addition, the band intensity at $3,447 \text{ cm}^{-1}$ decreased for Fe-IC500/6, it was attributed to the reduction of the surface hydroxyl group; which led to decrease of active sites on the adsorption of dye molecule onto the catalyst surface [10]. The incorporation of Fe ions into clay was illustrated with the disappearance and/or decrease in the intensities of bands at $800\text{--}900$ and $500\text{--}700 \text{ cm}^{-1}$ which are due to the deformation of Al_2OH and Si-O-Al [19,20].

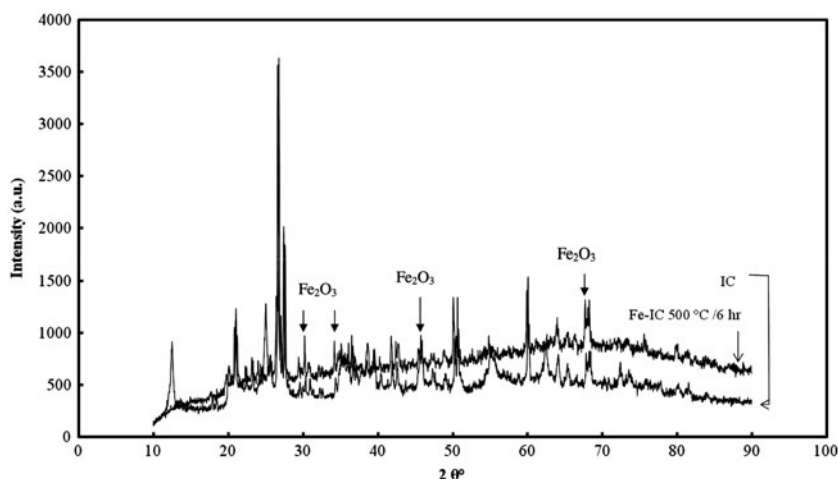


Fig. 2. XRD spectra of IC and Fe-IC500/6.

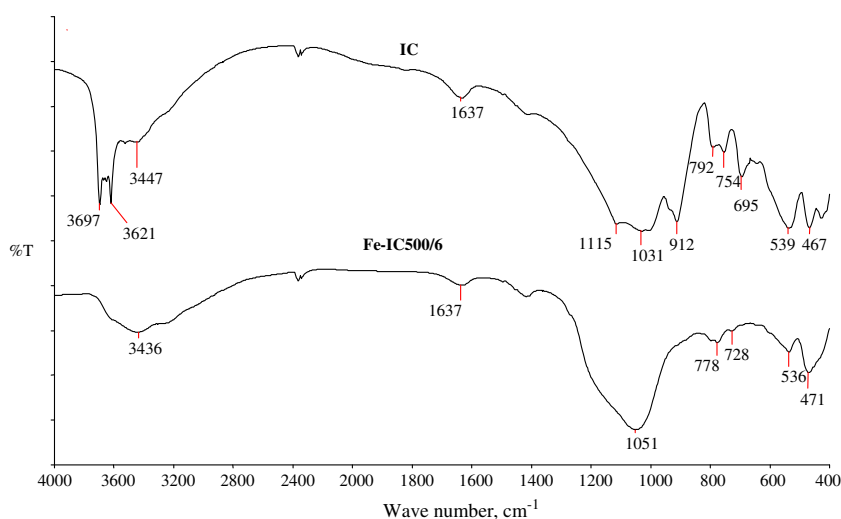


Fig. 3. FTIR spectra of IC and Fe-IC500/6.

3.2. Preliminary studies on the decolorization of AG25

The results of investigation of different participating mechanisms of AG25 decolorization are shown in Fig. 4. The AG25 decolorization with H_2O_2 (curve “a”) was carried out in blank solution without the addition of Fe-IC and it showed a negligible decolorization of less than 5% after 2 h. This was attributed to its low oxidation potential as compared with perhydroxyl or hydroxyl radicals [21]. However, when the solution pH was adjusted to pH 3 (curve “b”), decolorization of AG25 increased to 30% within the same reaction

time of 2 h. The results for the evaluation of influence adsorption process on AG25 decolorization by IC and Fe-IC are shown as curve “c” and “d”, respectively. The adsorptions of AG25 on IC and Fe-IC500/6 at pH 5.7 were less than 10 and 5%, respectively after 2 h. The decolorization efficiency under Fe-IC500/6 at pH 3 (curve “e”) was 27% and only 32% adsorption after 24 h (the figure not shown), while it was increased to 96% with the addition of H_2O_2 within the same reaction time (curve “f”). The results indicated that the decolorization of AG25 occurred predominantly with Fe-IC500/6 with H_2O_2 at pH 3.

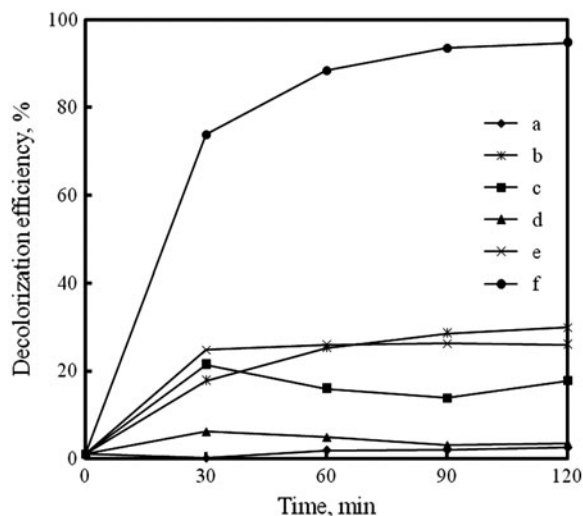


Fig. 4. AG25 decolorization through (a) H₂O₂, (b) H₂O₂ at pH 3, adsorption on (c) IC, (d) Fe-IC500/6, (e) Fe-IC500/6 at pH 3, and (f) Fenton process, Fe-IC500/6 with H₂O₂ at pH 3. Experimental conditions: (Initial concentration of AG25, [AG25]₀ = 50 mg/L; Fe-IC500/6 = 1.25 g/L, initial concentration of H₂O₂, [H₂O₂]₀ = 6.7 mM, Temperature, T = 30 °C, pH 5.7, and 130 rpm).

3.3. Effect of different parameters on the decolorization of AG25

3.3.1. Effect of catalyst calcination temperature and time duration on the decolorization of AG25 and its reusability

Another important quality of a good catalyst besides activity is its long-term stability. The long-term stability of catalyst accords it the ability to be used several times without losing its effectiveness. Fig. 5 shows the long-term stability of the different ranges of Fe-IC calcination temperature and time. The result indicated that Fe-IC400/6 had high percentage of AG25 decolorization at the first run which was 94% compared with other ranges of calcination temperature and time duration. However, during the second run, the percentage of AG25 decolorization by Fe-IC400/6 was decreased to 87%. This was similar with the decolorization of AG25 by Fe-IC400/4 and Fe-IC500/4 in the second run. In the third run, the decolorization of AG25 decreased gradually for all ranges of calcination temperature and the duration of time of Fe-IC, it was attributed to poisoning from adsorbed organic species on the active site and the iron ions leaching throughout the consecutive experiments [22]. But, among these ranges of catalyst calcination temperature and time duration, Fe-IC500/6 showed the smallest percentage reduction of AG25 decolorization from 80.7 to 79% in 1 h reaction time for the three

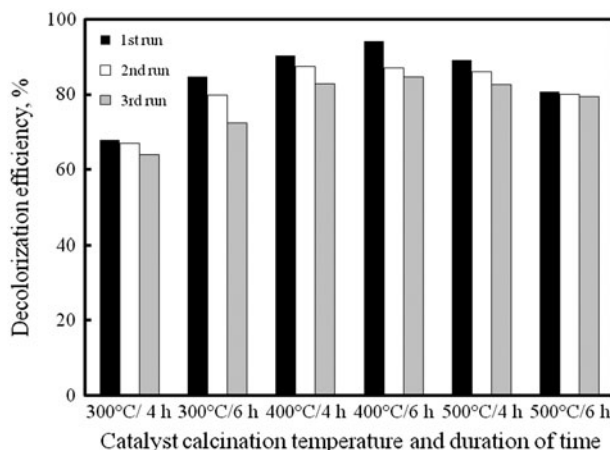


Fig. 5. Effect of catalyst calcinations temperature and time on the degradation of AG25. Experimental conditions: [AG25]₀ = 50 mg/L; [H₂O₂]₀ = 6.7 mM; Fe-IC = 1.25 g/L; T = 30 °C; pH 3 and 130 rpm.

runs; this was probably due to the stability of iron ions attached to the support. As the reaction time continued for 2 h, AG25 decolorization by Fe-IC500/6 was increased to 95% in first run, while 93% decolorization was obtained during the third run. The results connoted that the Fe-IC500/6 catalyst had an excellent long-term stability in the decolorization of AG25 and can be recycled more than three times with no drastic deactivation.

The concentration of iron ions leached from catalyst into the solution was measured after the decolorization of AG25 and the results are shown in Table 2. The most iron ions leaching into the solution were observed with the catalyst calcined at 400 °C for 6 h which was 0.4517 ppm of Fe. The concentration of iron ions leaching for all ranges of catalyst calcinations temperature and time was between 0.1746 and 0.4517 ppm in the dye solution, indicating that most of iron ions was retained in the solid phase catalyst with a negligible amount leaching into the solution. This is possibly due to the strong iron bond to support or engage in small oxide clusters dispersed in the solid, inside or outside the porosity. Najjar et al. [23] also reported that the parent compound also influences the complex mechanism of iron leaching. Fe-IC catalyst calcined at 500 °C for 6 h had the lowest leached Fe ions, even when it was subjected to reusability test it was found to be effective for three recycle times with almost negligible iron leaching from it. This temperature was agreed with some literature references which point out a range of 500–550 °C as being an optimal temperature for calcination process for clay support. Sum et al. [24] also found

Table 2
Iron leaching by different catalyst calcinations temperature and time

Catalyst samples	Fe concentration (ppm)
300°C 4 h	0.1746
300°C 6 h	0.3432
400°C 4 h	0.3465
400°C 6 h	0.4517
500°C 4 h	0.2772
500°C 6 h	0.2088

Experimental condition: $[AG25]_0 = 50 \text{ mg/L}$; hydrogen peroxide concentration = 6.7 mM; Fe-IC = 1.25 g/L; $T = 30^\circ\text{C}$; pH 3; 130 rpm.

that over 70% TOC removal of Acid Black 1 is obtained after 60 min by photo-Fenton reaction when the prepared catalyst is synthesized under the calcination temperature at 550°C .

3.3.2. Effect of pH on the decolorization of AG25

Many studies have reported that the pH of the solution markedly influences heterogeneous Fenton reactions as it controls the production rate of hydroxyl radical and the concentration of iron ions [18,21,25]. Therefore, a set of experiments were carried out by varying the initial solution pH from 2.5 to 5 to evaluate the influence of initial solution pH on the decolorization of AG25. As shown in Fig. 6, when the solution pHs were increased from 2.5 to 5, the decolorization of AG25 decreased from 98.9 to 35% after 120 min. This is due to the fact that at a high pH

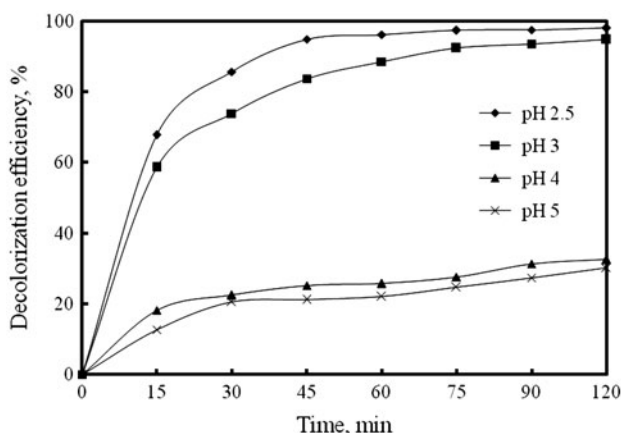


Fig. 6. Effect of pH on the decolorization of AG25. Experimental condition: $[AG25]_0 = 50 \text{ mg/L}$; $[H_2O_2]_0 = 6.7 \text{ mM}$; Fe-IC500/6 = 1.25 g/L; $T = 30^\circ\text{C}$, and 130 rpm.

value, H_2O_2 molecules started to decompose into molecular oxygen instead of hydroxyl radicals, resulting in the reduction of oxidative amounts [26]. Besides, this may be because at a lower pH value, more hydrogen ions (protons) were in the solution making the surface of the catalyst more positive thereby promoting electrostatic attraction activities between the negatively charged SO_3^- anion of the dye. Subsequently, the reaction of short-lived hydroxyl radicals with the dye molecules was enhanced due to the attraction of the dye molecules to the surface of the catalyst, thus increasing the AG25 decolorization rate. Similar trends were obtained by other researchers who ascribed the formation of complex irons which lead to the deactivation of the active site of the catalyst [27,28]. The decolorization efficiency of AG25 by Fe-IC500/6 was not much different between solution pH 2.5 and 3 at the end of the reaction process, which led to the selection of solution with pH 3 as the optimum solution pH throughout this study. This is because adjustment of solution pH to 2.5 will require more acid which subsequently translates to incurring more cost in the process.

3.3.3. Effect of catalyst dosage on decolorization of AG25

The effect of catalyst dosage of 0.75, 1.25, and 1.75 g/L on the decolorization of AG25 was investigated and the results are shown in Fig. 7. It was observed that increasing the catalyst dosage from 0.75 to 1.25 g/L, the dye decolorization increased from 79 to 95% after 2 h reaction. This was due to the increasing

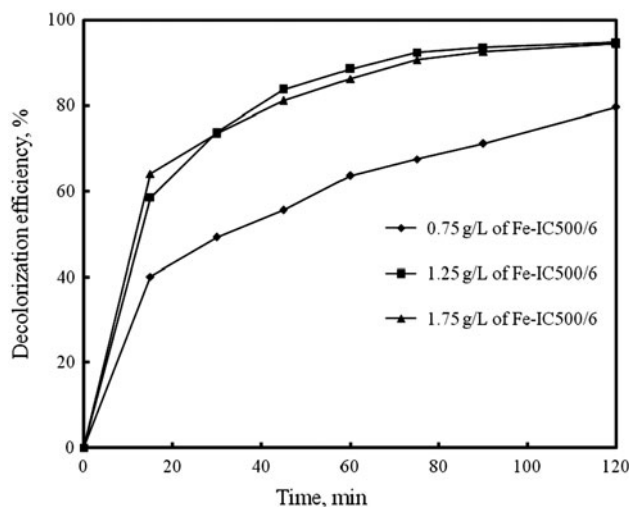
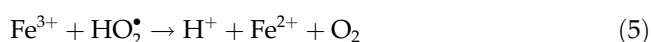


Fig. 7. Effect of catalyst dosage on the decolorization of AG25. Experimental conditions: $[AG25]_0 = 50 \text{ mg/L}$; $[H_2O_2]_0 = 6.7 \text{ mM}$; pH = 3; $T = 30^\circ\text{C}$, and 130 rpm.

amount of active sites for H_2O_2 decomposition. However, differences in terms of AG25 decolorization for catalyst dosage between 1.25 and 1.75 g/L were insignificant due to the development of parallel reactions as shown in Eqs. (2)–(5), as it has been widely observed in Fenton and Fenton-like processes. The parallel reactions were between the excess ferrous ions and either hydroxyl radicals, or with scavengers in the solution or other radicals present [29]:



3.3.4. Effect of $[\text{H}_2\text{O}_2]_0$ on the decolorization of AG25

The influence of initial concentration of hydrogen peroxide, $[\text{H}_2\text{O}_2]_0$ on the decolorization of AG25 was investigated and the results are shown in Fig. 8. It was observed that the decolorization efficiency increased from 91 to 96.6% after 2 h reaction with increasing $[\text{H}_2\text{O}_2]_0$ from 3.3 to 10 mM, but the decolorization of AG25 decreased upon further addition of the $[\text{H}_2\text{O}_2]_0$ from 13.3 to 17 mM. The increment of decolorization rate by the addition of $[\text{H}_2\text{O}_2]_0$ was due to increased decomposition of H_2O_2 into hydroxyl radicals. However, when the dosage of H_2O_2 was over

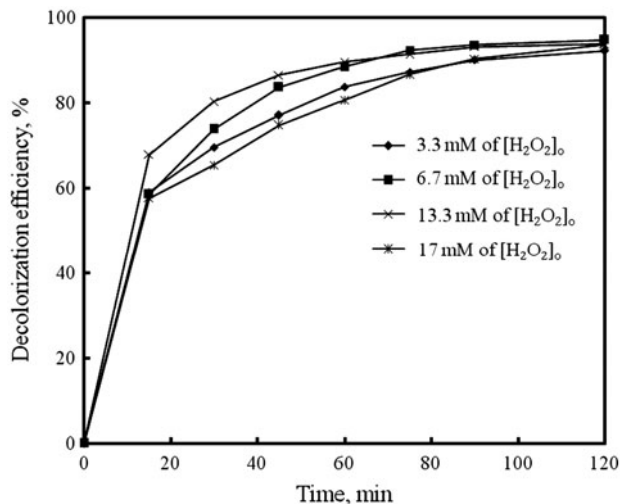


Fig. 8. Effect of $[\text{H}_2\text{O}_2]_0$ on decolorization of AG25. Experimental conditions: $[\text{AG25}]_0 = 50 \text{ mg/L}$; $\text{Fe-IC500/6} = 1.25 \text{ g/L}$; $T = 30^\circ\text{C}$; $\text{pH} = 3$, and 130 rpm.

17 mM, the decolorization of AG25 decreased slightly. It could be attributed to the formation of scavengers of hydroxyl radicals at higher concentrations of H_2O_2 , which led to a decrease in the concentration of hydroxyl radicals in the solution [30]. Further experiments were run by using 6.7 mM H_2O_2 due to its remarkable AG25 decolorization as compared with 13.3 mM, hence reducing chemical cost.

3.3.5. Effect of temperature on the decolorization of AG25

Fig. 9 depicts the influence of temperature in the range of 30–60°C on the decolorization of AG25 by Fe-IC500/6. The results revealed that higher temperatures increased decolorization efficiency of AG25; this was because the rate of generation of hydroxyl radicals was increased with temperature elevation [30]. The effect of temperature on the AG25 removal showed that at 30, 40, 50, and 60°C for 15 min reaction time, corresponding AG25 decolorization of 58, 73.4, 77.9, and 93.1% was recorded. A similar result has been reported for the increase of decolorization with increased temperature of the reaction [31].

3.3.6. Effect of initial dye concentration on the decolorization of AG25

Fig. 10 shows the decolorization of AG25 over time for four initial AG25 concentrations (10–100 ppm). It was observed that the initial dye concentration affects the decolorization efficiency of AG25. For example, decolorization efficiency of AG25 increases from about

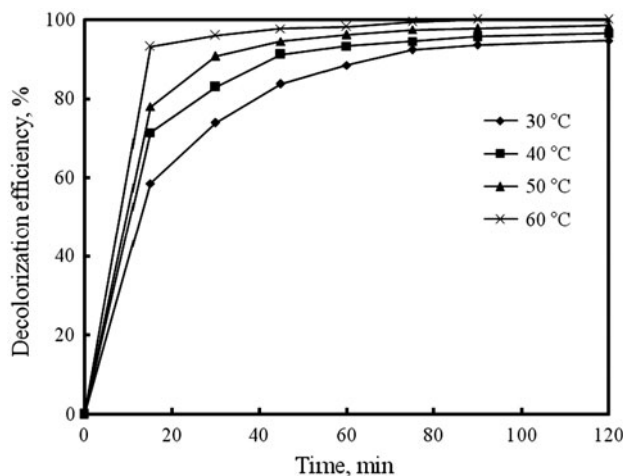


Fig. 9. Effect of temperature on the decolorization of AG25. Experimental conditions: $[\text{AG25}]_0 = 50 \text{ mg/L}$; $\text{Fe-IC500/6} = 1.25 \text{ g/L}$; $[\text{H}_2\text{O}_2]_0 = 6.7 \text{ mM}$; $\text{pH} = 3$ and 130 rpm.

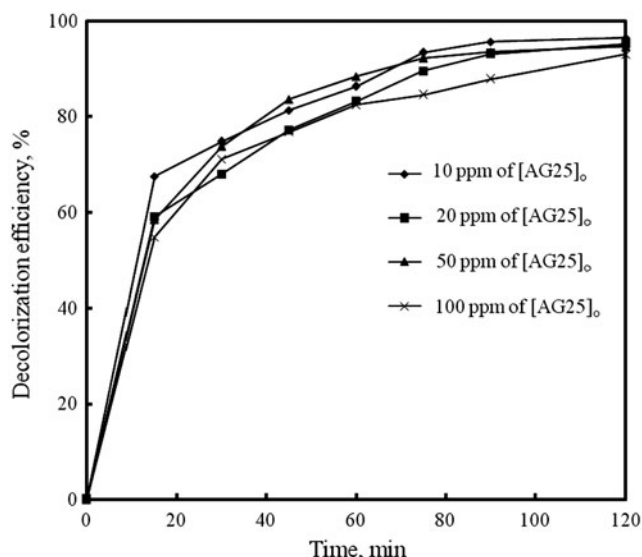


Fig. 10. Effect of initial dye concentration on the decolorization of AG25. Experimental conditions: Fe-IC500/6 = 1.25 g/L; $[\text{H}_2\text{O}_2]_0 = 6.7 \text{ mM}$; $T = 30^\circ\text{C}$; pH 3, and 130 rpm.

55.6% in 100 ppm to 68.9% in 10 ppm after 20 min of reaction. This is because as the concentration of AG25 increased, the number of AG25 molecules per volume unit was increased; therefore, more molecules of dye existed in solution while concentration of OH^\bullet remains unchanged. Furthermore, collision between dye molecules and OH^\bullet was reduced, leading to reduced decolorization rate of AG25 in the Fenton process [2]. However, it was observed that the decolorization efficiency for an initial dye concentration of 100 ppm was higher than 20 ppm initial concentration after 30 min reaction as well as AG25 decolorization efficiency of initial concentration of 50 ppm was higher than 10 ppm in 60 min reaction. This is because at higher initial dye concentrations, the quantity of dye molecules per volume unit is increased. Therefore, this enhances the probability of collision between short-lived OH^\bullet and reactant molecules, leading to an increase in the decolorization efficiency [27,32].

3.4. UV-vis spectra of the AG25 decolorization

UV-visible adsorption spectra of 50 mg/L AG25 were studied to investigate the decolorization of AG25 using Fenton process at the best experimental conditions (i.e. 1.25 g/L of Fe-IC500/6, 6.7 mM H_2O_2 , pH 3 at 30°C). The spectra of AG25 decolorization (Fig. 11(a)) were scanned in the range 700–290 nm which were characterized by two maximum absorbance peaks at 609 and 642 nm and another small peak at 409 nm in the visible region. A 298-nm band

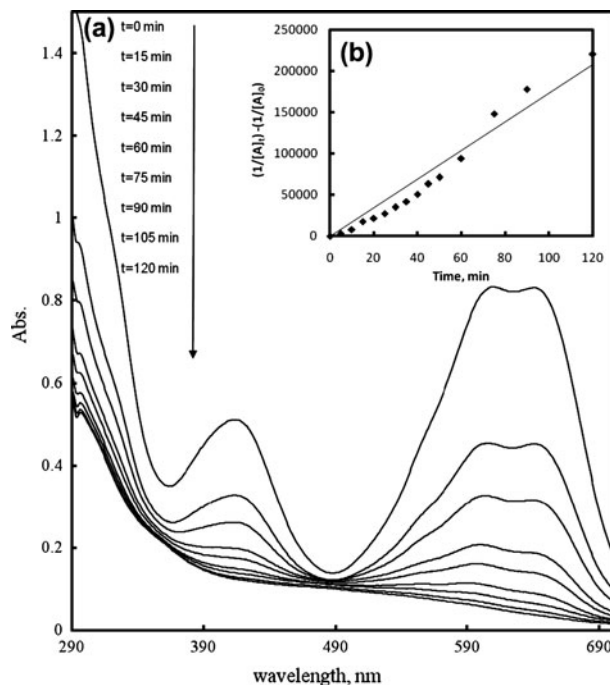


Fig. 11. (a) Absorbance spectra. (Experimental conditions: $[\text{AG25}]_0 = 50 \text{ mg/L}$; $[\text{H}_2\text{O}_2]_0 = 6.7 \text{ mM}$; Fe-IC500/6 = 1.25 g/L; pH 3; $T = 30^\circ\text{C}$ and 130 rpm. Inset: (b) the second-order linear relationship).

located in ultraviolet region was attributed to the benzene cycles substituted by SO_3^{2-} groups and to the anthraquinonic part [33]. The degradation of AG25 in solution caused a reduction in the absorbance in the visible part of the spectrum, whereas at shorter wavelengths attributed to benzene, it decreased slowly. Decolorization was fast during the first 45 min of the treatment which led to 83.4% degradation of AG25. Beyond this time, decolorization decreased slowly to 92.3, 93.5, and 95% in 75, 90 and 120 min, respectively. It was observed that the adsorption peaks at the visible region diminished very fast while adsorption peak at ultraviolet band vanished at lower rate. This means that the destruction of benzene and anthraquinone structure is very difficult. The decrease indicated that the formation of OH^\bullet radicals first attacks $-\text{N}-$ bond, destructing benzene and anthraquinone structure and hence causing decolorization [24]. From the change in the intensity of the maximum absorption peak located at 642 nm which is used to evaluate the decolorization rate of AG25, a pseudo-second-order kinetic analysis is obtained, as is depicted in the inset panel of Fig. 11(b). The rate constant of AG25 decolorization in the Fenton reaction is calculated to be $1,732 \text{ L mol}^{-1} \text{ min}^{-1}$ according to the slope and the equation of $1/[C]_t - 1/[C]_0 = kt$.

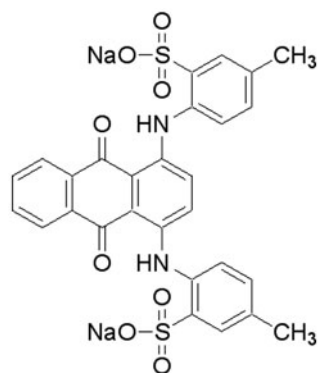


Fig. 12. Molecular structure of AG25.

However, even the complete decolorization of AG25 does not mean that AG25 is completely mineralized. Therefore, the analysis of AG25 mineralization using TOC was also studied at the best operating conditions (i.e. 1.25 g/L catalyst loading, 6.7 mM H_2O_2 , and pH 3 at 30°C). The percentage TOC removal of 50 ppm AG25 after a reaction time of 2 h was 78% and then increased to 85 and 90.1% after 3 and 4 h of reaction time, respectively. The TOC results showed that AG25 does not totally decompose into CO_2 and water. This is because the intermediate products formed during the process were difficult to oxidize within the specified time.

4. Conclusion

Ipoh clay was found to be a good locally sourced alternative catalyst that can be used in the Fenton process. Fe-IC calcined at 500°C for 6 h was the most efficient catalyst with 95% decolorization of AG25 for 2 h. In the batch process of decolorization of 50 ppm AG25 at 30°C, the best performance of Fe-IC500/6 was at pH 3, 1.25 g/L catalyst loading, and 6.7 mM of H_2O_2 . The Fenton treatment removed 78% of the AG25 within 2 h and this value increased to 85 and 90.1% after 3 and 4 h reaction time, respectively. This catalyst revealed an effective catalytic activity after three runs with 93% AG25 decolorization achieved in 2 h and, it also showed a negligible Fe leaching in Fenton-like processes. Therefore, Fe-IC is a promising catalyst for Fenton-like processes for AG25 decolorization.

Acknowledgments

The authors acknowledge the research grant from Universiti Sains Malaysia, under short-term grant (Project No 6039004) and also the financial support from National Science Fellowship (NSF), Ministry of Science, Technology and Innovation (MOSTI), Malaysia.

References

- [1] V. Kitsiou, N. Filippidis, D. Mantzavinos, I. Poullos, Heterogeneous and homogeneous photo catalytic degradation of the insecticide imidacloprid in aqueous solutions, *Appl. Catal. B* 86 (2009) 27–35.
- [2] F.L.Y. Lam, X. Hu, T.M.H. Lee, K.Y. Chan, A combined technique of photo-doping and MOCVD for the development of heterogeneous photo-Fenton catalyst, *Sep. Purif. Technol.* 67 (2009) 233–237.
- [3] Y.E. Benkli, M.F. Turan, M.S. Celik, Modification of organo-zeolite surface for the removal of reactive azo dyes in fixed-bed reactors, *Water Res.* 39 (2005) 487–493.
- [4] D. Hermosillaa, M. Cortijo, C.P. Huang, The role of iron on the degradation and mineralization of organic compounds using conventional Fenton and photo-Fenton processes, *Chem. Eng. J.* 155 (2009) 637–646.
- [5] P.X. Wu, Y. Li, N. Zhu, Z. Dang, Q. Chen, Heterogeneous photo-Fenton photodegradation of reactive brilliant orange X-GN over iron-pillared montmorillonite under visible irradiation, *J. Hazard. Mater.* 168 (2009) 901–908.
- [6] F. Martinez, G. Calleja, J.A. Melero, R. Molina, Heterogeneous phot-Fenton degradation of phenolic aqueous solution over iron-containing SBA-15 catalyst, *Appl. Catal. B* 60 (2005) 181–190.
- [7] W. Wang, M. Zhou, Q. Mao, J. Yue, X. Wang, Novel NaY zeolite-supported nanoscale zero-valent iron as an efficient-heterogeneous Fenton catalyst, *Catal. Comm.* 11 (2010) 937–941.
- [8] B. Muthukumari, K. Selvam, I. Muthuvel, M. Swaminathan, Photoassisted hetero-Fenton mineralization of azo dyes by Fe (II)- Al_2O_3 catalyst, *Chem. Eng. J.* 153 (2009) 9–15.
- [9] H.L. Wang, W.Z. Liang, Q. Zhang, W.F. Jiang, Solar-light-assisted Fenton oxidation of 2,4-dinitrophenol (DNP) using Al_2O_3 -supported Fe(III)-5-sulfosalicylic acid (ssal) complex as catalyst, *Chem. Eng. J.* 164 (2010) 115–120.
- [10] H. Hassan, B.H. Hameed, Fe-clay as effective heterogeneous Fenton catalyst for the decolorization of Reactive Blue 4, *Chem. Eng. J.* 171 (2011) 912–918.
- [11] B. Guadalupe, P. Ortiz de la, M.O. Alfano, E.A. Cassano, Optical properties of goethite catalyst for heterogeneous photo-Fenton reactions: Comparison with a titanium dioxide catalyst, *Chem. Eng. J.* 137 (2008) 396–410.
- [12] S.H. Tiana, Y.T. Tua, D.S. Chena, X. Chena, Y. Xiong, Degradation of Acid Orange II at neutral pH using $\text{Fe}_2(\text{MoO}_4)_3$ as a heterogeneous Fenton-like cataly, *Chem. Eng. J.* 169 (2011) 31–37.
- [13] T.L.P. Dantas, V.P. Mendonc, H.J. Jos, A.E. Rodrigues, R.F.P. M. Moreira, Treatment of textile wastewater by heterogeneous Fenton process using a new composite Fe_2O_3 /carbon, *Chem. Eng. J.* 118 (2006) 77–82.
- [14] R. Koswojo, R.P. Utomo, Y.H. Ju, A. Ayucitra, F.E. Soetaredjo, J. Sunarso, S. Ismadji, Acid Green 25 removal from wastewater by organo-bentonite from Pacitan, *Appl. Clay Sci.* 48 (2010) 81–86.
- [15] D. Fabbri, P. Calza, A.B. Prevot, Photoinduced transformations of Acid Violet 7 and Acid Green 25 in the presence of TiO_2 suspension, *J. Photochem. Photobiol. A: Chem* 213 (2010) 14–22.
- [16] C. Bouasla, M.E.-H. Samar, F. Ismail, Degradation of methyl violet 6B dye by the Fenton process, *Desalination* 254 (2010) 35–41.
- [17] J. Fernandez, J. Bandara, A. Lopez, P. Buffar, J. Kiwi, Photo-assisted Fenton degradation of non-biodegradable azo dye (Orange II) in Fe-free solutions mediated by cation transfer membranes, *Langmuir* 5 (1999) 185–192.
- [18] Q. Chen, P. Wu, Z. Dang, N. Zhu, P. Li, J. Wu, X. Wang, Iron pillared vermiculite as a heterogeneous photo-Fenton catalyst for photocatalytic degradation of azo dye Reactive Brilliant Orange X-GN, *Sep. Purif. Technol.* 71 (2010) 315–323.
- [19] N.K. Daud, B.H. Hameed, Fenton-like oxidation of Reactive Black 5 solution using iron Montmorillonite K10 catalyst, *J. Hazard. Mater.* 176 (2010) 1118–1121.

- [20] F.G.E. Nogueira, J.H. Lopes, A.C. Silva, M. Goncalves, A.S. Anastacio, K. Sapag, L.C.A. Oliveira, Reactive adsorption of Methylene Blue on montmorillonite via an ESI-MS study, *Appl. Clay Sci.* 43 (2009) 190–195.
- [21] E.G. Solozhenko, N.M. Soboleva, V.V. Goncharuk, Decolorization of azo-dye solutions by Fenton's oxidation, *Water Res.* 29 (1995) 2206–2210.
- [22] C. Catrinescu, M. Teodosiu, M. Macoveanu, J. Miehle-Brendle, R. Le Dred, Catalytic wet peroxide oxidation of phenol over Fe-exchanged pillared beidellite, *Water Res.* 37 (2003) 1154–1160.
- [23] W. Najjar, S. Azabou, S. Sayadi, A. Ghorbel, Toluene degradation in water using AlFe-Pillared clay catalysts, *Appl. Catal. B* 74 (2007) 1–6.
- [24] O.S.N. Sum, J. Feng, X. Hu, P.L. Yue, Pillared laponite clay-based Fe nanocomposites as heterogeneous catalysts for photo-Fenton degradation of acid black 1, *Chem. Eng. Sci.* 59 (2004) 5269–5275.
- [25] H. Katsumata, S. Kaneco, T. Suzuki, K. Ohta, Y. Yobiko, Degradation of linuron in aqueous solution by the photo-Fenton reaction, *Chem. Eng. J.* 108 (2005) 269–276.
- [26] M.A. Tarr, Fenton and modified Fenton methods for pollution degradation, In: M.A. Tarr (Ed), *Chemical Degradation Methods for Wastes and Pollutants-Environmental and Industrial Application*, Marcel Dekker Inc., New York, NY, 2003, pp. 165–200.
- [27] H. Hassan, B.H. Hameed, Oxidative decolorization of Acid Red 1 solutions by Fe-zeolite Y type catalyst, *Desalination* 276 (2011) 45–52.
- [28] Q. Chen, P. Wu, Y. Li, N. Zhu, Z. Dang, Heterogeneous photo-Fenton photo degradation of reactive brilliant orange X-GN over iron-pillared montmorillonite under visible irradiation, *J. Hazard. Mater.* 168 (2009) 901–908.
- [29] J.H. Ramirez, F.J. Maldonado-Hodar, A.F. Perez-Cadenas, C. Moreno-Castilla, C.A. Costa, L.M. Madeira, Azo-dye Orange II degradation by heterogeneous Fenton-like reaction using carbon-Fe catalysts, *Appl. Catal. Environ.* 75 (2007) 312–323.
- [30] J. Chen, I. Zhu, Heterogeneous UV-Fenton catalytic degradation of dyestuff in water with hydroxyl-Fe pillared bentonite, *Catal. Today* 126 (2007) 463–470.
- [31] J.H. Ramirez, C.A. Costa, L.M. Madeira, G. Mata, M.A. Vicente, M.L. Rojas-Cervantes, A.J. Lopez-Peinado, R.M. Martin-Aranda, Fenton-like oxidation of Orange II solutions using heterogeneous catalysts based on saponite clay, *Appl. Catal. B: Environment.* 71 (2007) 44–56.
- [32] N.K. Daud, M.A. Ahmad, B.H. Hameed, Decolorization of Acid Red 1 dye solution by Fenton-like process using Fe-Montmorillonite K10 catalyst, *Chem. Eng. J.* 165 (2010) 111–116.
- [33] M.R. Ghezzar, F. Abdelmalek, M. Belhadj, N. Bendorouche, A. Addou, Gliding arc plasma assisted photocatalytic degradation of anthraquinonic Acid Green 25 in solution with TiO₂, *Appl. Catal. B: Environment* 71 (2007) 304–332.